

Modelling Surface Energy Fluxes over Maize using Radiometric Soil and Canopy Temperature Observations.

Sánchez, Juan M.; Caselles, Vicente; Valor, Enric; Coll, César; Nicolòs, Raquel; Galve, Joan M. y Mira, María

Departamento de Física de la Tierra y Termodinámica, Facultad de Física, Universidad de Valencia.

C/ Dr Moliner N° 50, 46100, Burjassot, España.
juan.m.sanchez@uv.es

RESUMEN

En este trabajo mostramos una versión simplificada de un modelo de balance de energía de dos fuentes (STSEB), empleando un esquema desacoplado. Hemos aplicado el modelo STSEB a un amplio intervalo de proporciones de vegetación, usando datos de un cultivo de maíz. Comparando con las medidas realizadas desde una torre, hemos mostrado valores de RMSD entre 15 y 50 W m⁻² para la radiación neta y los flujos de calor en el suelo, sensible y latente. Hemos realizado un análisis de la sensibilidad del modelo a errores típicos en sus parámetros de entrada, mostrando errores relativos ~30% en la estimación de flujos de calor latente.

Palabras claves: STSEB, flujos de energía, temperaturas radiométricas.

ABSTRACT

A Simplified Two-Source Energy Balance (STSEB) model has been developed using a «patch» treatment of the surface flux sources. The feasibility of the STSEB approach under a full range in fractional vegetation cover conditions is explored using data from maize (corn) crop. Comparison with tower flux measurements yielded RMSD values between 15 and 50 W m⁻² for the retrieval of the net radiation, soil, sensible and latent heat fluxes. A sensitivity analysis of the STSEB approach to typical uncertainties in the required inputs showed relative errors reaching ~30% in latent heat flux estimates.

Keywords: STSEB, energy fluxes, radiometric temperatures.

Introduction

The estimation of surface energy fluxes using remote sensing techniques has been widely studied in recent years.

The development of two-source (soil + vegetation) layer models to accommodate partial canopy cover conditions considers energy exchange between soil and canopy components, and hence interaction between soil and canopy elements (Shuttleworth and Wallace, 1985). Another type of two-source model formulation is the so-called patch model where it is assumed that all the fluxes act vertically and that there is no interaction between soil and canopy com-

ponents (i.e., a complete energy balance between the atmosphere and each element; Blyth and Harding, 1995).

Norman et al. (1995) introduced a remote sensing-based two-source layer modelling framework for computing surface fluxes using directional brightness temperature observations. The Two-Source Energy Balance model (TSEB) was developed to require minimal inputs, similar to single-source models. Since typically only composite brightness temperature observations are available, an additional assumption is required for obtaining initial estimates of soil and vegetation canopy component temperatures and

energy fluxes. For the TSEB scheme, the Priestley-Taylor (PT) equation applied to the vegetated canopy is used to obtain an initial solution.

Alternatively, if the partitioning of composite land-surface temperature into soil and canopy temperatures is known a priori, e.g., through dual angle Thermal InfraRed (TIR) decomposition (e.g., François, 2002), the soil and canopy latent heat rates can be computed directly as a residual to the component energy budgets. In this case, the PT formulation is no longer required in the TSEB scheme.

In this paper a Simplified Two-Source Energy Balance (STSEB) model is developed, based on a patch representation of the energy exchange from soil and canopy, which permits estimation of surface fluxes under partial canopy cover conditions directly from component soil and canopy temperatures. A simple algorithm to predict the net radiation partitioning between soil and vegetation is also developed as part of the STSEB model.

The objective of this paper is to validate the STSEB model under variable conditions of vegetation cover, as well as to explore its sensitivity to the input uncertainties likely to typically occur at regional scales. Ground and tower-based remote sensing, vegetation cover and micrometeorological data from maize (corn) crop in an experimental field site in Beltsville Maryland, USA during the 2004 summer growing season were used.

Model description

The net energy balance of soil-canopy-atmosphere system is given by (neglecting photosynthesis and advection):

$$R_n = H + LE + G + F \quad (1)$$

where R_n is the net radiation flux ($W m^{-2}$), H is the sensible heat flux ($W m^{-2}$), G is the soil heat flux ($W m^{-2}$), and F is the rate of change of heat storage in the canopy layer ($W m^{-2}$). For short canopies, F can be neglected since its contribution to energy balance is usually quite small and difficult to reliably estimate with standard micrometeorological measurements. The effective radiometric surface temperature in the same system, T_R (K), can be obtained as a weighted composite of the soil temperature, T_s (K), and the canopy temperature, T_c (K):

$$T_R = \left[\frac{P_v(\theta)\epsilon_c T_c^4 + (1-P_v(\theta))\epsilon_s T_s^4}{\epsilon} \right]^{1/4} \quad (2)$$

where ϵ_c , and ϵ_s , are the canopy and soil emissivities, respectively, ϵ is the effective surface emissivity, and $P_v(\theta)$ is the fractional vegetation cover for the viewing angle θ . Note that equation (2) is based on the Stefan-Boltzmann law, and that interaction between soil and canopy components (cavity effect) is not accounted. $P_v(\theta)$ can be estimated from the measurements of Leaf Area Index (LAI) via:

$$P_v(\theta) = 1 - \exp\left(\frac{-0.5\Omega(\theta)LAI}{\cos(\theta)}\right) \quad (3)$$

where $\Omega(\theta)$ is a clumping factor to characterize the heterogeneity of the surface (Anderson et al. 2005). This factor makes it possible to extend the typical equations for random canopies to heterogeneous cases. The dependence of the clumping factor on θ can be estimated with:

$$\Omega(\theta) = \frac{\Omega_0 \Omega_{\max}}{\Omega_0 + (\Omega_{\max} - \Omega_0) \exp(\kappa \theta^p)} \quad (4)$$

where Ω_{\max} approaches unity for an azimuth view perpendicular to the crop row, and p and κ depend on stand architecture (Campbell and Norman, 1998).

The partitioning of the different fluxes into soil and canopy components was accomplished according to the scheme shown in Figure 1. According to this configuration, the addition between the soil and canopy contributions to the total sensible heat flux, H_s and H_c , respectively, are weighted by their respective partial areas as follows:

$$H = P_v H_c + (1 - P_v) H_s \quad (5)$$

where H_s and H_c are expressed as:

$$H_c = \rho C_p \frac{T_c - T_a}{r_a^h} \quad (6a)$$

$$H_s = \rho C_p \frac{T_s - T_a}{r_a^a + r_a^s} \quad (6b)$$

where ρC_p is the volumetric heat capacity of air ($J K^{-1} m^{-3}$), T_a is the air temperature at a reference height (K), r_a^h and r_a^a are the air aerodynamic resistances ($m s^{-1}$), and r_a^s is the soil aerodynamic resistance ($m s^{-1}$) (see details in Li et al. 2005).

To be consistent with the patch model configuration, a partitioning of the net radiation flux, R_n , between the soil and canopy is proposed as follows:

$$R_n = P_v R_{nc} + (1 - P_v) R_{ns} \quad (7)$$

where R_{nc} and R_{ns} are the contributions (values per unit area of component) of the canopy and soil, respectively, to the total net radiation flux. They are estimated by establishing a balance between the long-wave and the short-wave radiation separately for each component:

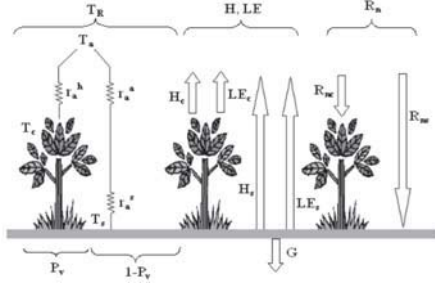


Fig. 1. Scheme of resistances and flux partitioning between soil and canopy, corresponding to the STSEB approach. Symbols are defined in the text.

$$R_{nc} = (1 - \alpha_c)S + \varepsilon_c L_{sky} - \varepsilon_c \sigma T_c^4 \quad (8a)$$

$$R_{ns} = (1 - \alpha_s)S + \varepsilon_s L_{sky} - \varepsilon_s \sigma T_s^4 \quad (8b)$$

where S is the solar global radiation ($W m^{-2}$), α_s and α_c are soil and canopy albedos, respectively, and σ is the Stefan-Boltzmann constant. L_{sky} is the incident long-wave radiation ($W m^{-2}$).

A similar expression to equation (5) is used to combine the soil and canopy contributions, LE_s and LE_c , respectively, to the total latent heat flux:

$$LE = P_v LE_c + (1 - P_v) LE_s \quad (9)$$

According to this framework, a complete and independent energy balance between the atmosphere and each component of the surface is established, from the assumption that all the fluxes act vertically. In this way, the component fluxes to the total latent heat flux can be written as:

$$LE_c = R_{nc} - H_c \quad (10a)$$

$$LE_s = R_{ns} - H_s - \frac{G}{(1 - P_v)} \quad (10b)$$

Finally, G can be estimated as a fraction (C_G) of the soil contribution to the net radiation (Choudhury et al. 1987):

$$G = C_G(1 - P_v)R_{ns} \quad (11)$$

This scheme is similar to a patch approach as there is weighting of the soil and canopy elements and no direct coupling is allowed between soil and vegetation. Moreover, The STSEB net radiation model does not consider attenuation of the downwelling sky and upwelling soil emission by an intervening canopy layer.

Because T_s and T_c can be estimated a priori from directional measurements of $T_{R'}$, or directly obtained through appropriate measurements of the separated components, the system of equations in the STSEB can be solved without using the Priestley-Taylor approach to provide an initial estimate of LE_c .

Study site and measurements

This work is based on the data registered in a corn crop field associated with the Optimizing Production Inputs for Economic and Environmental Enhancement (OPE3) program, located at the USDA-ARS Beltsville Agricultural Research Center, Beltsville, Maryland ($39^\circ 01'00''N$, $76^\circ 52'00''W$, 40 m above sea level). In this paper we will focus on the experimental campaign carried out in the summer of 2004, encompassing all the states in the growing season of the corn, from the beginning of June (plant emergence) to the end of July (cob formation). Corn was planted on May 18th in rows (N-S oriented) of 76-cm spacing.

Starting on June 9th, soil and canopy radiometric temperatures were measured simultaneously using Apogee IRTS-P3 infrared radiometers. This radiometer has a broad band (7-14 μm) with an accuracy of $\pm 0.3^\circ C$, and 37° field of view. Soil temperature was measured with an Infrared Thermometer (IRT) mounted in the center of a row at an oblique angle ($\sim 45^\circ$) viewing parallel to the row crop. Canopy temperature was sensed with a second IRT oriented horizontally viewing the plants parallel to the row orientation (Fig. 2a). Both temperature components were measured at two separated locations in the corn field, using two pairs of radiometers. Concurrently, the effective composite temperature of the corn+soil system was measured by a fifth IRT placed on a tower at 4.5 m height, viewing the surface at approximately a 45° viewing angle and an azimuth view perpendicular to the row direction. The micro-meteorological and eddy covariance instrumentation were mounted on the same 10-m tower (Fig. 2b).

Net radiation was measured with a Kipp & Zonen CNR-1 net radiometer at 4.5 m above ground level (agl). This net radiometer measures separately the incoming and outgoing short-wave and long-wave radiation components. Six

REBS soil heat flow transducers (HTF-1) were buried 8-cm below the soil surface. Soil temperatures were measured at 2 and 6-cm depth by two Type-T soil thermocouples to compute the storage component of the soil heat flux above the plates. A Campbell Scientific 3-D sonic anemometer and LiCor 7500 water vapour/carbon sensor positioned at 4-m agl was used to measure momentum, sensible heat, latent heat and carbon fluxes, as well as wind speed and direction. Air temperature and vapour pressure was measured using a CSI HMP 45C sensor at 4-m agl. The sampling frequency was 10 Hz for the eddy covariance and 10 s for the energy balance and meteorological instrumentation. All data were stored as 30-minute averages on Campbell CR5000 and 23x data loggers.

Crop geometry and LAI were sampled periodically during corn development. The LAI estimates were made using a LiCor LAI 2000 instrument.

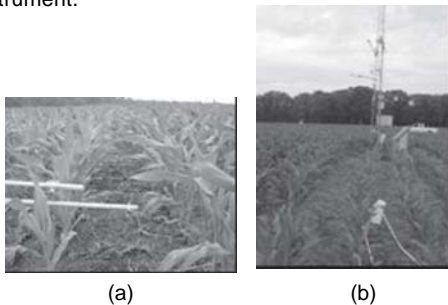


Fig. 2. (a) Experimental assembly of two Apogee IRTS-P3 infrared radiometers to measure T_c and T_s . (b) General view of the target and the micro-meteorological tower on which the instrumentation was mounted

Results and discussion

Radiometric measurements

As a first step, all the Apogee IRT measurements were corrected for emissivity and atmospheric effects using the radiative transfer equation, adapted to ground measurements. Atmospheric profiles from radiosoundings launched in an area nearby the study site were introduced into the MODTRAN 4 code to get estimates of the downwelling sky radiance for the atmospheric correction. Values of $\bar{\alpha}_c=0.985\pm 0.011$ and $\bar{\epsilon}_s=0.960\pm 0.013$ were used to estimate T_c and T_s , respectively (Rubio et al. 2003). To obtain values of T_c and T_s that are more representative of the whole corn field, averages between the

two different measurement locations were used. T_r estimated from the measurements of T_c and T_s is compared to direct observations from the tower-based radiometer. A standard error of ± 1.4 °C and a bias of 0.02 °C were obtained, supporting the assumption that temperature components, T_c and T_s , from the radiometric observations are representative of the effective soil and canopy temperatures in the flux footprint area surrounding the tower and thus can be employed with the STSEB model for computing the fluxes.

Validation of the STSEB model

Almost 1700 observations, without any exclusion related to time of day or sky conditions, were used to run and evaluate STSEB model output. However, the daytime flux statistics, are more descriptive of overall model utility and therefore these are discussed in the text below.

For estimating net radiation, Equations (7), (8a) and (8b) were applied using values of $\alpha_s=0.12$, $\alpha_c=0.20$, $\epsilon_s=0.960$, and $\epsilon_c=0.985$, characteristic of a corn canopy (Campbell and Norman, 1998). The model reproduces measured net radiation with good accuracy, yielding a bias of 8 W m^{-2} , and $\text{RMSD}=18 \text{ W m}^{-2}$ (Fig 3a). A constant value of $C_g=0.35$ was used in equation (11), corresponding to midway between its likely limits (Choudhury et al., 1987). Soil heat flux results overestimate measurements by 17 W m^{-2} on average, with $\text{RMSD}=43 \text{ W m}^{-2}$ (Fig. 3b).

Tables 1 list statistics comparing turbulent fluxes estimates of H and LE with the eddy covariance fluxes in their original form (EC), and corrected for closure using the residual (RE) and Bowen ratio (BR) techniques (Twine et al. 2000). The RE closure technique, using H_{EC} and assigning all closure error to LE (LE_{RE}), yields the best agreement between STSEB and measured fluxes.

Model comparisons with H_{EC} and LE_{RE} are shown in Fig 3c-d. Comparisons between modelled and measured H show a negative bias of -3 W m^{-2} , and a RMSD of 22 W m^{-2} (Fig. 3c). The slope (a) of a linear regression between STSEB H and H_{EC} is 0.86, indicating that the bias is multiplicative.

For LE there is a tendency to overestimate the observed latent heat flux, LE_{EC} with a slope of 1.04 and a $\text{RMSD}=62 \text{ W m}^{-2}$. This overestimation observed in the LE results may be due to an under-measurement problem with the eddy covariance system. The agreement of the LE results improves significantly when the RE closure technique is applied to the observations, decreasing the slope to 0.98 and the RMSD to 51 W m^{-2} (see Fig 3d and Table 1).

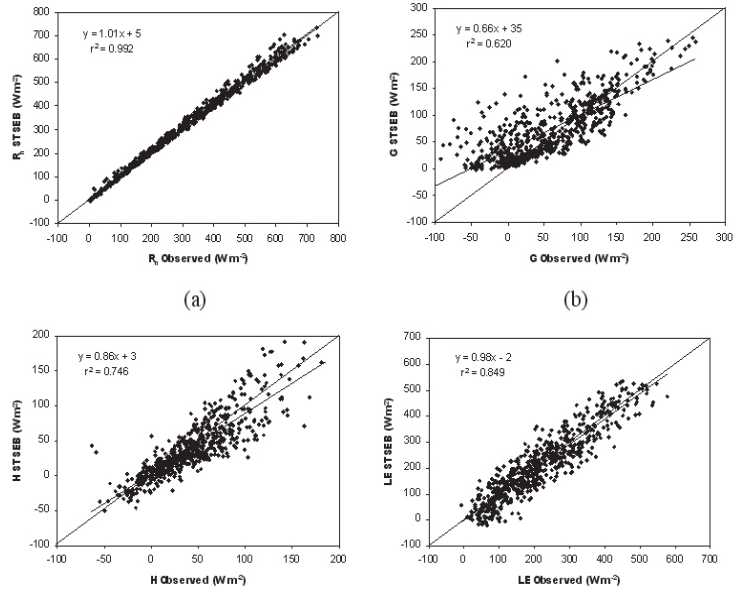


Fig. 3. Linear regressions between the surface energy fluxes estimated by the STSEB model versus their corresponding ground measured values: (a) R_n , (b) G , (c), H (eddy-covariance measurements), (d) LE (RE technique applied).

Table 1. Statistical analysis of the STSEB model performance with the daytime OPE3-2004 dataset.

Flux	Bias ($W m^{-2}$)	RMSD ($W m^{-2}$)	MAD ($W m^{-2}$)	a	b ($W m^{-2}$)	r^2
R_n	8	18	13	1.01	5	0.992
G	17	43	31	0.66	35	0.620
H_{EC}	-3	22	16	0.86	3	0.746
H_{BR}	-10	26	19	0.76	2	0.738
LE_{EC}	29	62	49	1.04	22	0.820
LE_{RE}	-6	51	40	0.98	-2	0.849
LE_{BR}	0	49	40	1.00	0.6	0.854

Comparison with the TSEB Model

To assess the impact of the simple patch approach used in the STSEB model in comparison with the layer configuration in the TSEB model, the TSEB was also applied to the OPE3 dataset from 2004. The TSEB was restructured to operate similarly to the STSEB, using observed values of soil and canopy component temperature and thereby eliminating the need for an initial PT approximation for potential canopy transpiration.

Statistics comparing this version of the TSEB (TSEB_comp) with observed daytime fluxes (corrected for closure using the residual method) are provided in Table 2. In general, there is good agreement between STSEB and TSEB_comp output as well as similar statistical results with the flux observations (cf. Table 1 and 2). The simple patch formulation for net radiation contained in the STSEB model, performs almost as well as the more detailed two-stream representation in the TSEB_comp under this set of conditions. It appears the patch modelling scheme is appropriate under the set of environmental conditions analyzed in this study.

Table 2. Statistical analysis of the TSEB_comp model performance with the daytime OPE3-2004 dataset. Statistical analysis of the STSEB model performance with the daytime OPE3-2004 dataset.

Flux	Bias (W m ⁻²)	RMSD (W m ⁻²)	MAD (W m ⁻²)	a	b (W m ⁻²)	r ²
R_n	-2	11	8	0.97	8	0.997
G	17	38	29	0.67	35	0.713
H_{EC}	-13	25	19	0.73	-1.7	0.737
LE_{RE}	-5	43	34	0.93	9	0.879

Sensitivity analysis of the STSEB model

For operational monitoring over regional scales, using satellite-derived inputs and non-local meteorological data, the typical uncertainties in the inputs for STSEB may lead to significant errors in estimated fluxes. To assess the impact of typical errors in remotely derived model inputs, a sensitivity analysis of the STSEB approach was performed following the method suggested by Zhan et al. (1996). The relative sensitivity, S_p , of a model flux estimate, Z , to X uncertainties in a parameter p , can be expressed as:

$$S_p(X) = \left| \frac{Z_- - Z_+}{Z_0} \right| \quad (12)$$

where Z_0 , Z_+ , and Z_- are the fluxes (H , R_n , or LE) predicted when p equals its reference value p_0 , when p is increased by X its reference value, and when p is decreased X its reference value, respectively, with all other input parameters held constant at their reference values.

In this analysis, all hourly daytime data were used as sets of reference values; hence a wide range of input values were considered. For each input variable, the time-series simulation was then performed using perturbed values of that variable, and S_p was averaged over the entire time series.

A list of all variables and parameters required by the STSEB model, as well as their assigned uncertainties, are provided in Table 3. Relative sensitivity values, S_p , estimated for some of these parameters can be artificially high in the case of H , due to low values of the reference flux. Since a major objective is in modelling vegetation stress and water use, the analysis also considered the sensitivity of R_n and LE to input errors.

Average S_p values for the whole experimental period are listed in Table 3 for the three fluxes, with values greater than 10% denoted in bold to indicate parameters that have a significant effect on the flux retrieval. Errors in soil, canopy, and air temperatures clearly have the greatest impact on the modelled sensible heat flux. Uncer-

tainty in other parameters such as soil and canopy emissivity values, canopy height, or wind speed also have a measurable effect on H . For R_n , incoming shortwave and long-wave radiation are the key inputs that lead to sensitivities greater than 10%. These radiation inputs, together with the soil, canopy and air temperatures, have the greatest effect on LE retrieval. For LE , all inputs have S_p values below 25% on average.

Figure 4 shows variations in model sensitivity with fractional vegetation cover condition. The S_p data were grouped in eight bins of width 0.1 in P_v , giving a range from 0.1 to 0.8. Average relative sensitivity values were computed for each P_v bin. Results for H , R_n , and LE are plotted in Figures 4a-4c, respectively. Inputs with S_p values lower than 10^{-3} are not shown. For model inputs related to the soil (T_s , α_s , and β_s), S_p decreases as P_v increases, whereas for those directly related with the canopy, such as T_c , ϵ_c , and μ_c , an increase in S_p is observed. For variables related to canopy structure such as LAI, canopy height and clumping, the relative sensitivity also increases as a function of P_v .

For latent heat flux estimation under low vegetation cover conditions ($P_v < 0.2$), the STSEB model is most sensitive to uncertainties in T_s , and under high vegetation cover conditions ($P_v > 0.6$) to uncertainties in T_c and T_a (Fig. 4c). The sensitivity of the STSEB model to any of the assumed uncertainties in the required inputs for the LE retrieval is less than 35% for the whole range of P_v . The sensitivity is even lower for the fractional vegetation cover range $0.3 < P_v < 0.6$, which yields S_p values less than 20%. Simulations in the estimation of soil and canopy temperatures from directional radiative temperature observations performed by François et al. (2002) covering a wide range of vegetation cover and moisture conditions showed that the error on T_s retrieval increases with increasing LAI, while the error on retrieved T_c generally decreases. If this behaviour were taken into account, the estimated uncertainties in the flux estimates might be reduced.

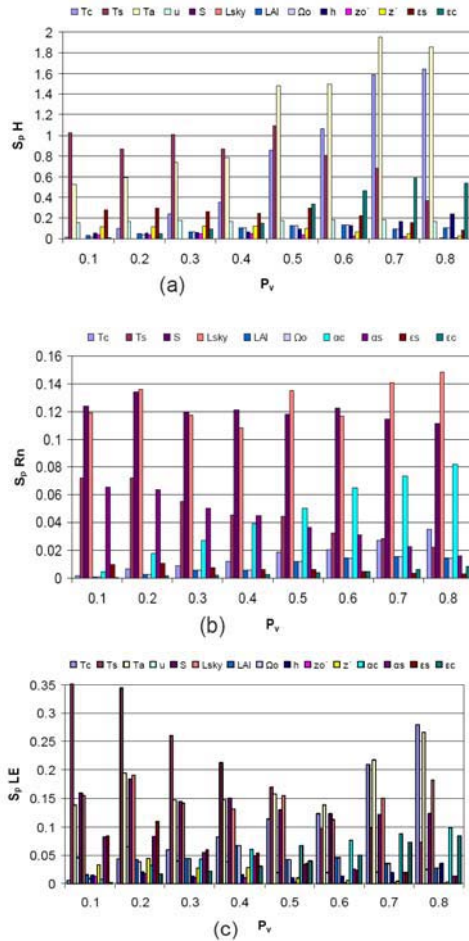


Fig. 4. Evolution of the relative sensitivity of the STSEB model to the different required inputs, S_p , with the vegetation cover, P_v , for: (a) H , (b) R_n , (c) LE .

Conclusions

A Simplified Two-Source Energy Balance model (STSEB) has been proposed to estimate surface fluxes over sparse canopies from the radiometric soil and canopy temperatures. The advantage of the present patch modelling approach is that it is a simplified version of the TSEB model, particularly in the way the net radiation is partitioned between the soil and vegetation.

On the other hand, the STSEB requires input measurements of canopy and soil temperature, while the TSEB performs an internal decomposition of a bulk surface radiometric temperature observation. The STSEB model has been tested under a full range of crop cover conditions using field data from a corn field at the USDA-ARS OPE3 experimental site in Beltsville Maryland, USA.

Radiometric soil and canopy temperatures were measured separately, and their reliability as representative component temperatures to be used as input to the STSEB model has been evaluated by comparing an independent tower-based radiometric temperature measurement of the effective composite temperature with that estimated from the two components. A $\text{RMSD} = \pm 1.4^\circ\text{C}$ between these two estimates of the effective composite temperature was observed.

The validation of the STSEB approach, using measurements of daytime surface energy fluxes, yields errors between $15\text{--}50\text{ W m}^{-2}$ for R_n , G , H , and LE after correcting the observed fluxes for closure. Reasonable agreement was obtained between the STSEB and a version of the TSEB model constructed to use component temperature data.

The operational capability of the STSEB model has been explored by means of an analysis of the sensitivity of the model flux output to uncertainties in the required inputs. The input temperature data, T_c , T_s , and T_a are shown to have the greatest impact on the STSEB estimate of the fluxes. Under the conditions considered in this study, much of the available energy was converted to latent heat, LE . As a result, the sensitivity of the STSEB model output in H to uncertainties in air, soil and canopy temperatures often exceeded 100% of its reference value. On the other hand, sensitivity of the STSEB model output in LE to these temperature uncertainties was generally less than 30% and not strongly a function of the vegetation cover over the range $0.1 < P_v < 0.8$.

In summary, these results demonstrate the utility of the STSEB model for a corn crop over a full range in cover conditions when reliable measurements of soil and canopy temperatures are available.

Table 3. Average values of the relative sensitivity, S_p , of the STSEB model to the uncertainties, X , in the required inputs for estimating H , R_n , and LE (description of results in italics in the manuscript).

INPUT	T_c (°C)	T_s (°C)	T_a (°C)	u (m s ⁻¹)	S (W m ⁻²)	L_{sky} (W m ⁻²)	LAI	Ω_0	h (m)	α_c	α_s	ϵ_c	ϵ_s
X	1 °C	2 °C	1 °C	10%	5%	5%	20%	20%	10%	20%	20%	0.02	0.02
H	0.66	0.86	1.10	0.17	0.0018	0.0018	0.08	0.07	0.10	<10 ⁻³	<10 ⁻³	0.24	0.23
R_n	0.015	0.05	0	0	0.12	0.13	0.008	0.008	0	0.04	0.04	0.003	0.007
LE	0.10	0.23	0.17	0.04	0.14	0.15	0.03	0.03	0.018	0.05	0.05	0.04	0.05

Acknowledgements

This work was funded by the *Ministerio de Educación y Ciencia* (Project CGL2004-06099-C03-01, co-financed with European Union FEDER funds, *Acciones Complementarias* CGL2005-24207-E/CLI and CGL2006-27067-E/CLI), and the University of Valencia (*V Segles* Research Grant of Mr. J. M. Sánchez). The authors would like to thank the logistical support in operating and maintaining the OPE3 site as well as data collection and archiving efforts of Drs. Craig Daughtry, Timothy Gish and Greg McCarty of the USDA-ARS Hydrology and Remote Sensing Lab. The micrometeorological tower data and vegetation were made available through the efforts of technician Mr. Andrew Russ of the Hydrology and Remote Sensing Lab and Dr. John Prueger from the USDA-ARS Soil Tilth Lab in Ames, Iowa. Funds from the USDA-ARS Hydrology and Remote Sensing Lab help support Mr. J. M. Sánchez as a visiting scholar.

References

Anderson, M.C., Norman, J.M., Kustas, W.P., Li, F., Prueger, J.H., and Mecikalski, J.R. 2005. Effects of vegetation clumping on two-source model predictions of surface energy fluxes from an agricultural landscape during SMA-CEX. *Journal of Hydrometeorology*, 6: 892-909.

Blyth, E. M., and Harding, R. J. 1995. Application of aggregation models to surface heat flux from the Sahelian tiger bush. *Agricultural and Forest Meteorology*, 72: 213-235.

Campbell, G. S., and Norman, J. M. 1998. *An introduction to Environmental Biophysics*, Springer, New York, 286 pp.

Choudhury, B. J., Idso, S. B., and Reginato, R. J. 1987. Analysis of an empirical model for soil heat flux under a growing wheat crop for estimating evaporation by an infrared-temperature based energy balance equation.

Agricultural and Forest Meteorology, 39: 283-297.

François, C. 2002. The potential of directional radiometric temperatures for monitoring soil and leaf temperature and soil moisture status. *Remote Sensing of Environment*, 80: 122-133.

Li, F., Kustas, W. P., Prueger, J. H., Neale, C. M. U., and Jackson, J. J. 2005. Utility of Remote Sensing Based Two-Source Energy Balance Model Under Low and High Vegetation Cover Conditions. *Journal of Hydrometeorology*, 6 (6): 878-891.

Norman, J. M., Kustas, W., & Humes, K. 1995. A two-source approach for estimating soil and vegetation energy fluxes from observations of directional radiometric surface temperature. *Agricultural and Forest Meteorology*, 77: 263-293.

Rubio, E., Caselles, V., Coll, C., Valor, E., and Sospedra, F. 2003. Thermal infrared emissivities of natural surfaces: improvements on the experimental set-up and new measurements. *International Journal of Remote Sensing*, 20 (24): 5379-5390.

Shuttleworth, W., & Wallace, J. 1985. Evaporation from sparse crops: an energy combination theory. *Quarterly Journal of the Royal Meteorological Society*, 111: 1143-1162.

Twine, T. E., Kustas, W. P., Norman, J. M., Cook, D. R., Houser, P.R., Meyers, T. P., Prueger, J. H., Starks, P. J., and Wesely, M. L. 2000. Correcting eddy-covariance flux underestimates over a grassland. *Agricultural and Forest Meteorology*, 103 (3): 279-300.

Zhan, X., Kustas, W. P., and Humes, K. S. 1996. An intercomparison study on models of sensible heat flux over partial canopy surfaces with remotely sensed surface temperature. *Remote Sensing of Environment*, 58: 242-256.